Dielectron production in proton-proton and proton-deuteron collisions at 1-2 GeV

A. I. Titov*

Department of Physics, National Taiwan University, Taipei, Taiwan 10764, Republic of China

B. Kämpfer[†]

Research Center Rossendorf, Institute for Nuclear and Hadron Physics, PF 510119, 01314 Dresden, Germany

E. L. Bratkovskaya[‡]

Bogoliubov Theoretical Laboratory, Joint Institute for Nuclear Research, 141980 Dubna, Russia

Estimates of elementary cross sections for dielectron production in pN and pd reactions are presented. Throughout, we use the vector dominance model for all hadron-hadron-photon vertices. The Δ, η Dalitz decays and bremsstrahlung appear as dominant sources of dielectrons. We show that the recently observed strong enhancement from 2 of the ratio of dielectron production from pd to pp collision at low energy $E \sim 1.0$–1.3 GeV may be understood by a different threshold behavior of eta production in proton-proton and proton-neutron collisions. Relying on a realistic deuteron wave function we estimate the energy dependence of the ratio and find qualitative agreement with new experimental results.

PACS number(s): 24.10.−i, 24.90.+d

I. INTRODUCTION

The available experimental data [1–3] on dielectron production in proton-proton or proton-nucleus or nucleus-nucleus collisions at 1–5 A GeV bombarding energies have stimulated a series of theoretical investigations [4–13] of the elementary production process. The reasons for this interest are obvious. Dielectrons are thought to represent one of the promising signals which can directly probe the dense and hot nuclear matter produced in heavy-ion collisions at intermediate energies. The reliable description of various elementary reaction channels for dielectron production serves as an input to theoretical models and event generators for simulating heavy-ion collisions. These simulations are needed to unfold dielectron spectra and to get the wanted information about compressed and heated nuclear matter. Also, via the dielectron decay channel of vector mesons one can probe the behavior of such mesons in an excited nuclear environment. The second-generation precision spectrometers are devoted to these investigations.

The theoretical investigations mentioned of the elementary production mechanisms of dielectrons in pN

reactions have stepwise improved the understanding of the relevant basis processes [4–14]. These investigations have interest in their own right also, with respect to new hadron facilities (e.g., COSY in Jülich), which are devoted to deeper insight into the hadron structure, hadronic reactions, and photon-hadron interactions. Concerning dielectron production, the models, with appropriate parametrization, are in satisfactory agreement with available experimental data [3] which still have low statistics. New data with high statistics are expected in the near future. Then theoretical estimates and underlying assumptions can be tested better since they depend on certain model parameters which are difficult to fix without experimental data. For example, in dielectron processes the off-shell behavior of the strong interaction part is probed in a wider kinematic regime than in the case of real photon bremsstrahlung or elastic scattering of hadrons or light nuclei. The timelike (half off-shell) form factor of the nucleon is still unknown in the region where the transfer momentum is near the vector meson masses. Details of certain channels, e.g., $pn \to \eta X$, are rather unsettled and reliable data do not yet exist. The latter fact is partially related to the difficulty in geting reliable information on pn reactions, in general, via light nuclei by subtracting masking many-body effects.

The aim of the present paper is to reestimate dielectron production cross sections in elementary nucleon-nucleon subprocesses and to apply them in pp and pd reactions at 1–2 GeV and explain the observed enhancement of the ratio of dielectron production in pd and pp collision at 1.0–1.3 GeV. We rely here on the vector dominance model (VDM) that has proven to be a useful guiding principle for hadron-photon interactions [15]. The VDM form factor has been implemented, e.g., in Ref. [14] and has been found to give reasonable results only if nuclear mat-

---

*Permanent address: Bogoliubov Theoretical Laboratory, Joint Institute for Nuclear Research, 141980 Dubna, Russia. Also at the Research Center Rossendorf, Institute for Nuclear and Hadron Physics PF 510119, 01314 Dresden, Germany. Electronic address: atitov@thsun1.jinr.dubna.su

[†]Also at the Institute for Theoretical Physics (KAI e.V.), Technical University, Dresden, Mommsenstr. 13, Germany. Electronic address: kaempfer@gamma.fz-rossendorf.de

[‡]Electronic address: brat@thsun1.jinr.dubna.su

ter corrections are taken properly into account. However, in the pp, pd, and p–light-nuclei reactions such a nuclear correction is not operative, and one has to implement the VDM form factor in an alternative way [16]. Here, we present a detailed study of the underlying microscopy in elementary subprocesses [12] of dielectron production in nucleon-nucleon collisions.

Remember that at 1–2 GeV the main dilepton sources are the following: $\pi^+\pi^-$ annihilation, $\pi^0, \Delta, \eta, \omega$ Dalitz decays, pN bremsstrahlung, and direct vector meson decays. For pp and pd reactions, when focusing on dileptons with invariant masses in the range of 0.15–0.9 GeV, only Δ, η, ω Dalitz decays and pN bremsstrahlung are important.

The Δ Dalitz decay is one of the strongest dilepton channels. In Refs. [5,6,13,14], it is used within a model where the Δ-production cross section in pN collisions is taken as a constant at fixed kinetic energy and is independent of the momentum transfer to the target nucleon, which is related to the Δ mass directly. Experimental data [17,18] and theoretical models [19], however, show such a dependence: the Δ-production cross section decreases with increasing values of the momentum transfer. The maximum of the dilepton invariant mass depends directly on the Δ mass and, therefore, one can expect some dynamical suppression of dileptons at large invariant masses. We find that, in spite of this suppression, it is almost compensated by the VDM form factor enhancement; the form of the spectra changes, and they obtain a resonancelike behavior at invariant masses near the rho-meson mass.

The analysis of the pN bremsstrahlung contribution in most previous papers is practically based on the so-called soft photon approximation. The soft photon approximation includes several approximations. A few of them are acceptable (e.g., keeping only the electric part of the hadron current and neglecting radiation from the virtual propagators and vertices), while others (e.g., integration over the unobservable phase space kinematical region) result in an overestimation of the cross section. This overestimation is sometimes corrected by a phase space volume reduction factor [5]. Here, we improve this approach by correct phase space integration.

A further problem concerns the pp bremsstrahlung contribution. It is usually assumed that, because of destructive interference of direct and exchanged amplitudes of the electric part of the bremsstrahlung matrix element, the amplitudes compensate each other. But that is not correct exactly, especially for high energy. The calculation of pp bremsstrahlung at 4.9 GeV in the soft photon approximation of Ref. [13] shows that it may overestimate the pn bremsstrahlung. So one expects only partial compensation of the electric part and both the pn and pp contributions should be taken into account. This conclusion is confirmed also in a recent paper [16] where both the proton-nucleon bremsstrahlung and the delta Dalitz decay are considered simultaneously within an effective one-boson exchange model.

Another strong source of dileptons is the η Dalitz decay. Most interesting here is the dilepton production near 1 GeV. The threshold energy for η production is about

1.26 GeV, and in pp collision this channel is suppressed kinematically. For pd collisions, however, it is open, but one has to deal carefully with the mechanisms of subthreshold η production.

These are the main items we are going to analyze in some detail. Our paper is organized as follows. In Sec. II, we analyze the Dalitz Δ-decay rate. In Sec. III, we discuss pn and pp bremsstrahlung contributions in pd reactions within the soft photon approximation for the electromagnetic hadron current but with exact multiple integration of the resulting squared matrix element. In Sec. VI we discuss the contribution of the η, ω Dalitz decays. In Sec. V, we present the calculated cross sections of various reaction channels and compare the dilepton production in pp and pd interactions. A summary is given in Sec. VI.

II. DALITZ DELTA DECAY

The cross section of the delta Dalitz decay is represented as follows:

$$\frac{d\sigma}{dM^2}^{\Delta \to e^+e^-N} = \int_{(m_N+m_\pi)^2}^{(\sqrt{s}-m_N)^2} dM_\Delta^2 \, \tilde{\sigma}_\Delta(s,M_\Delta)$$
$$\times D(M_\Delta) \frac{1}{\Gamma_\Delta} \left(\frac{d\Gamma}{dM^2}\right)^{\Delta \to e^+e^-N}, \quad (1)$$

where

$$\tilde{\sigma}_\Delta(s,M_\Delta) = \frac{1}{16\pi s(s-4m_N^2)}$$
$$\times \int_{t_{\min}(M_\Delta)}^{t_{\max}(M_\Delta)} dt \, |T_\Delta(s,t,M_\Delta)|^2 \quad (2)$$

and M_Δ and Γ_Δ are the mass and total width of an intermediate delta; T_Δ stands for the delta production matrix element, t denotes, as usual, the squared momentum transfer at the $NN \to \Delta N'$ vertex, and $\left(d\Gamma/dM^2\right)^{\Delta \to e^+e^-N}$ describes the differential width of the delta decay into a dilepton with invariant mass M. The "weight function" $D(M_\Delta)$ is proportional to the squared Δ propagator which leads to the relativistic Breit-Wigner form

$$D(M_\Delta) = \frac{1}{\pi} \frac{M_\Delta \Gamma_\Delta}{(M_\Delta^2 - M_{\Delta 0}^2)^2 + M_\Delta^2 \Gamma_\Delta^2} \quad (3)$$

with the mean value of $\langle M_\Delta \rangle = M_{\Delta 0} = 1.232$ GeV/c^2.

The simplest form of the $\Delta N\pi$ vertex is described by the interaction Lagrangian

$$\mathcal{L}_{\Delta N\pi} \sim \bar{\psi}_N(p_n)\psi_\Delta^\mu(P_\Delta)k_\mu\varphi(k), \quad (4)$$

where $\psi_N(p_n), \psi_\Delta^\mu(P_\Delta), \varphi(k)$ are the nucleon, delta, and pion wave functions, respectively, and k_μ denotes the pion four-momentum. Direct evaluation of the decay matrix element leads to a mass dependence of the Δ width in Eq. (3),

$$\Gamma_\Delta(M_\Delta) = C \frac{(M_\Delta + m_N)^2 - m_\pi^2}{M_\Delta^2} |\mathbf{k}|^3. \tag{5}$$

Here $\mathbf{k}$ denotes the c.m. momentum in the πN channel, and the constant C is determined by the condition $\Gamma_\Delta(M_{\Delta 0}) = 110$ MeV. The dependence $\Gamma_\Delta(M_{\Delta 0})$ in Eqs. (3) and (5) differs from the corresponding ones used in Ref. [6]; however, both of them coincide at the few percent level.

The Δ-decay probability $(d\Gamma/dM^2)^{\Delta \to e^+ e^- N}$ is calculated on the basis of the $\Delta N\gamma$-interaction Lagrangian

$$\mathcal{L}_{\Delta N\gamma} = eF_\gamma(M^2)\bar{\psi}_\Delta^\beta \Gamma_{\beta\mu}\psi_N A^\mu, \tag{6}$$

where A^μ denotes the electromagnetic four-potential, and $F_\gamma(m^2)$ is the vector dominance timelike electromagnetic form factor. For baryons this form factor in the kinematical region is still unknown. Following the vector dominance principle we use the minimal way to incorporate it: we assume that this form factor has a unique form for all hadrons, that is, we use the $\pi\pi\gamma$ VDM form factor. The physical meaning of this is quite clear: the virtual photon interacts with the pion cloud surrounding the nucleons and deltas. We employ the experimentally established parametrization [4]

$$F_\gamma^2(M^2) = \frac{m_\rho^4}{(M^2 - m_\rho'^2)^2 + (m_\rho \Gamma_\rho')^2}, \tag{7}$$

with $m_\rho' = 761$ MeV and $\Gamma_\rho' = 118$ MeV; the vertex function $\Gamma_{\beta\mu}$ (6) is taken from Ref. [20]. The result of a direct calculation may be written as

$$\frac{1}{\Gamma_\Delta}\frac{d\Gamma}{dM^2}^{\Delta \to e^+ e^- N} = \frac{\alpha}{3\pi M^2}B_\gamma^\Delta(M_\Delta)R_\gamma^\Delta(M_\Delta, M),$$

$$R_\gamma^\Delta(M_\Delta, M) = \frac{\Gamma^{\Delta \to \gamma^* N}(M_\Delta, M)}{\Gamma^{\Delta \to \gamma N}(M_\Delta, 0)}. \tag{8}$$

Here $B_\gamma^\Delta(M_\Delta)$ stands for the branching ratio of the electromagnetic width to the total delta decay width $[B_\gamma^\Delta(M_\Delta = 1.232 \text{ GeV}) \simeq 0.6 \times 10^{-2}]$, R_γ^Δ is the ratio of the electromagnetic delta-decay widths for virtual to real photons,

$$R_\gamma^\Delta(M_\Delta, M) = \frac{M_\Delta M^2 + 5M_\Delta q_0^2 - 3M^2 m_N - 3M^2 q_0 - 3m_N q_0^2 - 3q_0^3}{q_0^2(5M_\Delta - 3m_N - 3q_0)}$$

$$\times \left[\lambda(M_\Delta^2, m_N^2, M^2)/\lambda(M_\Delta^2, m_N^2, 0)\right]^{1/2}, \tag{9}$$

and $q_0 = (M_\Delta^2 + M^2 - m_N^2)/(2M_\Delta)$, $\lambda(x, y, z) = x^2 + y^2 + z^2 - 2(xy + yz + xz)$.

For the calculation of the t-integrated cross section $\tilde{\sigma}_\Delta(s, M_\Delta)$ in Eq. (2), we adopt the one-pion exchange model. By straightforward calculation we find the Δ production matrix element in the form

$$\hat{T}_\Delta = a \frac{(\bar{\psi}_\mu^\Delta \tau_1 \psi_{N_1} k^\mu)(\bar{\psi}_{N'}\gamma_5\gamma^\nu \tau_2 \psi_{N_2} k_\nu)}{k^2 - m_\pi^2}$$

$$\times \frac{\Lambda_{NN\pi}^2 - m_\pi^2}{\Lambda_{NN\pi}^2 - k^2}\frac{\Lambda_{\Delta N\pi}^2 - m_\pi^2}{\Lambda_{\Delta N\pi}^2 - k^2}, \tag{10}$$

where $m_\pi = 140$ MeV/c, and k_μ is the four-momentum of the exchanged pion. The constant a is determined by the normalization condition

$$\int_{(m_N + m_\pi)^2}^{(\sqrt{s} - m_N)^2} dM_\Delta^2 \; \tilde{\sigma}_\Delta(s, M_\Delta)D(M_\Delta) = \sigma_\Delta(s). \tag{11}$$

In the above formula $\sigma_\Delta(s)$ stands for the Δ-production cross section which we take as a product of the well-known analytical parametrization of the Δ-production cross section of Ver West and Arndt [21], σ_Δ^{V-A}, and the "high energy" correction factor

$$\sigma_\Delta(s) = \sigma_\Delta^{V-A}\frac{\theta(E - E_0)}{1 + A(E - E_0)^2}, \tag{12}$$

where $E_0 = 1.3$ GeV, $A = 0.5$ GeV^{-2}, and E is the projectile kinetic energy in the laboratory system. The correction factor in Eq. (12) is introduced to ensure the reproduction of experimental data above E_0.

The t-integrated Δ-production cross section $\tilde{\sigma}_\Delta$ in

Eq. (1) at fixed $\sigma_\Delta(s)$ depends on the cutoff parameters $\Lambda_{NN\pi}, \Lambda_{\Delta N\pi}$ in Eq. (10), which should be fitted to the differential cross section of the delta production. The result is more sensitive to the model at lower energies ($E \sim$1–2 GeV) and large dielectron invariant masses (near the threshold). Figure 1 shows the result of the fitting procedure for the $pp \to n\Delta^{++}$ reaction at initial
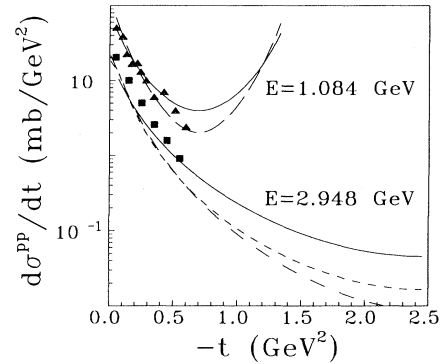
FIG. 1. Elastic Δ-production cross section for the $pp \to \Delta^{++}n$ reaction at bombarding energies 1.084 and 2.948 GeV. Experimental data at 1.084 (triangles) are taken from Ref. [17], while data at 2.948 GeV (squares) are from Ref. [18]. The solid lines correspond to calculations with the T matrix (10) and $\Lambda_{NN\pi} = \Lambda_{N\Delta\pi} = 0.7$ GeV. The curves representing calculations at 2.948 GeV correspond to the usage of the T matrix from Ref. [19] with $\Lambda_{NN\pi} = \Lambda_{N\Delta\pi} = 0.545$ GeV (long dashes) and to the exploiting of the T matrix (10) with $\Lambda_{NN\pi} = \Lambda_{N\Delta\pi} = 0.545$ GeV (dashes). At 1.084 GeV both the latter curves practically coincide (very long dashes).

kinetic energies 1.084 and 2.948 GeV. The solid lines correspond to the exclusive delta-production cross section with the T matrix of Eq. (10) with $\Lambda_{NN\pi} = \Lambda_{N\Delta\pi} = 0.7$ GeV. We calculate the spin averaged squared matrix element using the relativistic Rarita-Schwinger propagator for spin 3/2 particles. The long dashed lines correspond to the calculation with the T matrix taken from Ref. [19] taking into account the short-range correlations and cutoff parameters $\Lambda_{NN\pi} = \Lambda_{N\Delta\pi} = 0.545$ GeV (set D of Ref. [19]). A similar result comes from the T matrix of Eq. (10) with the same cutoff parameters (see the dashed lines in Fig. 1). At higher energies, one can see that the predictions for these two last models practically coincide, while in the high-t region they differ from the calculation with the cutoff parameters $\Lambda \simeq 0.7$ GeV. This difference is also seen in the delta Dalitz decay rate in pp interactions at 1 and 2 GeV shown in Fig. 2. The short dashed lines represent the calculation with a constant t-weighted Δ-production cross section in Eq. (1) while the other lines correspond to the different Δ-production T matrices (with the same notation as in Fig. 1). One can see that at 1 GeV the M_Δ dependence of the t-weighted cross section in Eq. (2) suppresses the delta Dalitz decay rate by a factor of 2 at $M \sim 0.35$ GeV. The differences coming from different T matrix parametrizations are below 50%. At 2 GeV, the suppression is even larger, a factor of ~ 7 at $M \sim m_\rho$. The difference between different models for the T matrix may amount to a factor of 2. Therefore, for a clear understanding of the Δ Dalitz decay rate, more detailed data on the differential delta-production cross section at large momentum transfer are necessary. In the subsequent calculations we will use the delta-production T-matrix as in Eq. (10) with $\Lambda_{NN\pi} = \Lambda_{N\Delta\pi} = 0.7$ GeV, which seems to be preferable to reproduce the known experimental data on the delta-production cross section.

III. BREMSSTRAHLUNG DILEPTON PRODUCTION

Dilepton radiation via pn bremsstrahlung has been extensively studied, cf. Refs. [4,5,10,11,22]. Explicit diagrammatic calculations of the pn bremsstrahlung are performed on the basis of the one-boson exchange model [10,16,22,23] where four mesons $(\pi, \sigma, \omega, \rho)$ are used for the description of the two-body pn T matrix. It is found that the result depends on the two-body T matrix parameters which cannot be fixed uniquely only by fitting to the pn elastic scattering. This method is too complicated to be used as a convenient input in many-body kinetic calculations of dilepton production in nucleus-nucleus collisions. As has been mentioned in the Introduction, to avoid these difficulties a method based on the soft photon approximation [5] has been used in Refs. [6,7,14]. One should keep in mind that the soft photon approximation contains at least three approximations: (i) it keeps only the electric part of the electromagnetic current, (ii) it neglects the radiation from the internal charged meson exchange lines and the nucleon-nucleon-meson vertices, and (iii) it contains an approximate integration over unobservable kinematic variables, where the momentum, energy, and invariant mass of the virtual photon are assumed to be negligible as compared to the other variables (e.g., the initial and momentum transfer, etc.). The comparison with the exact diagrammatic calculation [10,22,23] shows that the first two approximations change the result not more than a few percent and really may be approved. But the third approximation appears crude. To improve the result, a phenomenological reduction factor has been introduced in Ref. [5], which is aimed to reduce the remaining phase space volume for the colliding hadrons in their final state. We must stress that this factor cannot be extracted explicitly from a multidimensional integral, and one should be careful in interpreting the final result within this model, especially at large invariant dilepton masses. For all these reasons, in the present paper we use a model that employs the first two approximations (i) and (ii) of the soft photon approximation; however, it takes into account exact kinematic relations. The net result reads

$$\frac{d\sigma_{ab \to e^+ e^- a'b'}}{dM}$$

$$= \frac{\alpha^2}{16^2\pi^4} \frac{1}{M^3\sqrt{s(s - 4m_N^2)}} F_\gamma^2(M) \, F_\gamma^2(M)$$

$$\times \int dy \, dq_\perp^2 \, dE_b' \, d\varphi \, \frac{1}{|\mathbf{q}|} \, J_\mu \, J_\nu \, \mathcal{P}^{\mu\nu}, \tag{13}$$
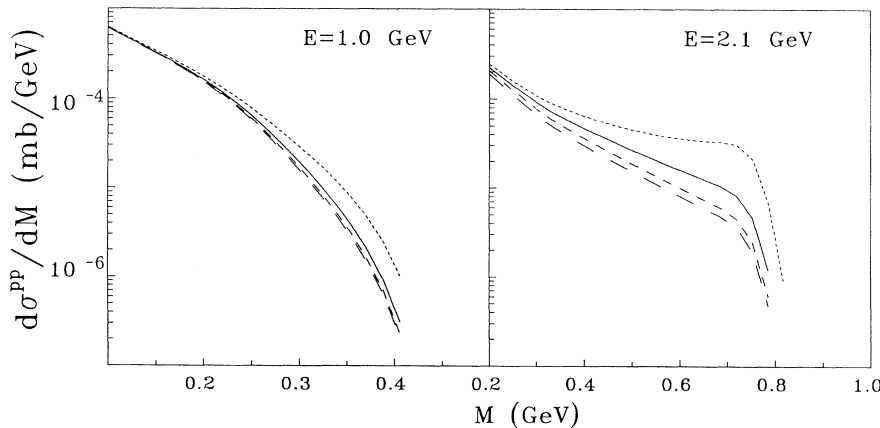
FIG. 2. The Dalitz delta-decay contribution to the dielectron production at E = 1 and 2.1 GeV. The results of calculations with the constant production cross section $\tilde{\sigma}_\Delta(s, M_\Delta)$ in Eq. (1) are represented by the lines with short dashes while other lines correspond to different Δ-production T matrices. Notation is the same as in Fig. 1.

where $\mathcal{P}^{\mu\nu} = -\frac{4}{3}(g^{\mu\nu}q^2 - q^\mu q^\nu)$ is a projector, and J^μ is the hadron current. The upper and lower limits of the integral over dE'_b are defined from the condition

$$|\cos\theta_{\mathbf{q},\mathbf{p}'_b}| = \left| \frac{s - 2\sqrt{s}q_0 + M^2 - 2(\sqrt{s} - q_0)E'_b}{2|\mathbf{q}||\mathbf{p}'_b|} \right| \leq 1. \tag{14}$$

Let us first discuss the structure of the hadron current. For the pn bremsstrahlung in the soft photon approximation it has the usual form

$$J^\mu_{pn} = -\frac{p^\mu_a}{p_a q}\mathcal{T}(s', t, (p_a - q)^2) + \frac{p'^{\,\mu}_a}{p'_a q}\mathcal{T}(s, t, (p'_a + q)^2), \tag{15}$$

which is gauge invariant in the on-shell limit

$$\mathcal{T}(s', t, p^2) = \mathcal{T}(s, t, m^2_N), \tag{16}$$

with

$$|\mathcal{T}(s, t, m^2_N)|^2 = 16\pi s(s - 4m^2_N)\frac{d\sigma}{dt}^{ab\to a'b'}(s, t), \tag{17}$$

where p_a and p'_a are the four-momenta of the initial and outgoing protons; $\mathcal{T}$ is the strong interaction two-body T matrix; $t = (p_b - p'_b)^2 = 2m^2_N - 2E_b E'_b + 2|\mathbf{p}_a||\mathbf{p}'_b|(\cos\theta_{\mathbf{q},\mathbf{p}_a}\cos\theta_{\mathbf{q},\mathbf{p}'_b} + \sin\theta_{\mathbf{q},\mathbf{p}_a}\sin\theta_{\mathbf{q},\mathbf{p}'_b}\cos\varphi)$, $s = (p_a + p_b)^2$, and $s' = (p_a + p_b - q)^2$. $(d\sigma/dt)^{ab\to a'b'}(s, t)$ denotes the elastic $ab \to a'b'$ scattering cross section; the symbol a denotes a proton and b refers to a neutron.

The electric part of the hadron current in a pp collision within the soft photon approximation takes the form

$$J^\mu_{pp} = -\frac{p^\mu_a}{p_a q}\mathcal{T}(s', t) - \frac{p^\mu_b}{p_b q}\mathcal{T}(s', t')$$
$$+\frac{p'^{\,\mu}_a}{p'_a q}\mathcal{T}(s, t) + \frac{p'^{\,\mu}_b}{p'_b q}\mathcal{T}(s, t'). \tag{18}$$

Here p_a and p_b are the four-momenta of the projectile and target proton, and $t' = (p_b - p'_b - q)^2$. It is seen that the hadron current J^μ_{pp} (18) does not vanish at finite values of q_0 and M.

One of the still open and interesting questions here is the off-shell corrections to this process. Each of the T matrices in Eqs. (15) and (18) are far off shell with $\sum m^2_i \neq m^2_N$, where m_i ($i = a, b, a', b'$) is the mass of interacting particles. If we describe the nucleon-nucleon interaction on the basis of the effective one-boson exchange T matrix, we have to introduce vertex form factors, which, for the on-shell case, depend only on the squared momentum transfer t. For the "one half" on-shell T matrix, we have in the bremsstrahlung process also effective vertex functions that must depend on an additional invariant variable. The squared momentum p^2 of the off-shell nucleon may be chosen as this variable. For a qualitative analysis we can use also the dimensionless off-shell variable $\xi = p^\mu p_\mu/m^2_N$, where m_N is the nucleon mass and p^μ denotes the four-momentum of the virtual off-shell proton after or before photon radi-

ation. A kinematic analysis shows that, for large values of invariant masses as well as for high energies and momenta of the virtual photon, ξ is far from its on-shell value $\xi = 1$. A phenomenological analysis of the off-shell correction to the effective one-boson exchange T matrix is performed in Ref. [12] where some additional off-shell suppression of the bremsstrahlung rate at higher energy is introduced. This suppression depends on the value of a dimensional cutoff parameter which should range on a typical hadron scale 1–2 GeV. Unfortunately, till now we have not at hand an appropriately well-founded generic theoretical model for the off-shell T matrices and form factors. In order to avoid in the present consideration such an additional parameter, in our further calculations we use the on-shell model and put in Eqs. (15) and (18) $t' = t$ and $s' = s$, which are expected to give an upper estimate of the bremsstrahlung contribution. The procedure of including the off-shell dependence into the electromagnetic form factors and two-body T matrices is discussed in [16]. But the concrete calculation in [16] is performed with the on-shell form factors, and the final results of Ref. [16] and our approach are very close to each other.

Figure 3 shows separately the contribution of the pp and pn bremsstrahlung at 1 GeV. One can see that at 1 GeV the pp contribution is about 30–40 % of the pn bremsstrahlung. For comparison, we also present the result of calculation of the pn bremsstrahlung within the traditional soft photon approximation [5]:

$$\frac{d\sigma}{dM}^{pn\to e^+e^-p'n'}$$

$$= \frac{\alpha^2}{6\pi^2 M} F^2_\gamma(M) \int dy\, dq^2_\perp\, dt \left(\frac{-t}{m^2_N q^2_0}\right)$$
$$\times \frac{d\sigma}{dt}^{pn\to p'n'}(s, t)\, \frac{R_2(s')}{R_2(s)}, \tag{19}$$

where R_2 is the Lorentz invariant two-body phase space integral of the final two nucleons of energy $\sqrt{s}$. In calculation of Eq. (19) the expression for the pn elastic cross
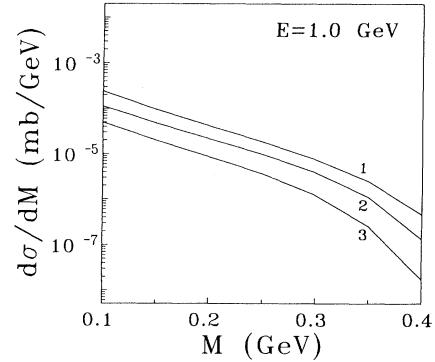
FIG. 3. Contributions of the pn (curve 2) and pp (curve 3) bremsstrahlung to the dielectron production at 1 GeV. The curve 1 represents a contribution of the pn bremsstrahlung calculated within the soft photon approximation [see Eq. (19)].

section is taken the same as in Eq. (15). One can see that the soft photon approximation with a phase space correction results in a twice larger cross section than taking into account the explicit conservation law in calculations.

Another essential effect is the interference of the bremsstrahlung and delta Dalitz decay channels [16]. However, this effect depends strongly on the model for the two-body T matrix. If we use the one-boson exchange model with the four mesons then we would require 12 energy dependent parameters which in principal cannot be uniquely determined only from the elastic NN scattering. This is the main reason why we use the soft photon approximation with effective two-body T matrix, which is proportional to the square root of the elastic NN scattering cross section. We lose the phases and lose the interference terms. This is the price for the inadequate knowledge of the nucleon-meson dynamics in the GeV region.

One more interesting effect is the bremsstrahlung in the $pp \to p\Delta$ reaction. In Ref. [16] it is taken into account simultaneously with the $pN \to pN$ channel; in our case this channel should be investigated independently. We plan to investigate this point in our future work.

In all our calculations we use an energy dependent parametrization for the elastic pp and pn cross sections. The corresponding parameters are found by standard fitting to the known experimental data. These cross sections decrease with increasing energy, which leads to a decrease of the bremsstrahlung rate in the total dilepton production. In the pd interaction the pn and pp contributions are summed coherently.

IV. MESON DALITZ DECAY

The contribution of the η Dalitz decay takes the form

$$\frac{d\sigma}{dM^2}^{\eta \to e^+ e^- \gamma} = \sigma_{pd \to \eta X}(s) \frac{2\alpha}{3\pi M^2} 0.39 \; F_\gamma^2(M)$$
$$\times \left(\frac{\lambda(m_\eta^2, M^2, m_0^2)}{\lambda(m_\eta^2, 0, m_0^2)} \right)^{3/2}, \quad m_0 = 0,$$
(20)

where the number 0.39 is the branching ratio for the $\eta \to \gamma\gamma$ decay [24]. When calculating the η production in pd scattering, we use a realistic deuteron wave function ϕ_d obtained within the Paris potential model [25]

$$\sigma_{pd \to \eta X}(s) = \int \mathcal{R} \left[\sigma_{pp \to \eta pp}(s'(k)) + \sigma_{pn \to \eta pn}(s'(k)) \right]$$
$$\times |\phi_d(\mathbf{k})|^2 \, d\mathbf{k},$$
(21)

where $\mathbf{k}$ is the relative nucleon momentum in the deuteron, and $\mathcal{R}$ denotes the flux factor. The internal nucleon motion in the deuteron is important near and below the η threshold. We also include short-range correlations describing a simultaneous interaction of the proton with a correlated two-nucleon cluster in the deuteron wave function with a 5% probability, as in Ref. [26]. Such an effect has been found important for scattering processes near thresholds and at large angles [26–28]. In

the present calculation, the η-production cross section is taken in the form

$$\sigma_{pd \to \eta X}(s) = (1 - \alpha)\sigma_{pd \to \eta X}^{(1)}(s) + \alpha \sigma_{pd \to \eta X}^{(2)}(s),$$
(22)

where α is the correlation probability ($\alpha = 0.05$) and $\sigma^{(1)}$ is determined by Eq. (21), while $\alpha\sigma^{(2)}$ is the contribution of the correlated two-nucleon cluster, which we will discuss later.

The cross section for the η production in pp collisions via the intermediate $N^*(1535)$ resonance has been studied within the one-boson exchange model in Refs. [29,30]. The results of those calculations depend on the input parameters and are different in the two papers just near the threshold. The assumption that the threshold behavior of the η-production cross section in the collision of particles a and b is mainly determined by the phase space integral results in

$$\sigma_{ab \to \eta ab}(s) \sim \sqrt{\frac{m_a m_b (m_a + m_b) m_\eta}{\lambda(s^2, m_a^2, m_b^2)}} \left(1 - \sqrt{\frac{s_0}{s}}\right)^2,$$

$$s_0 = (m_a + m_b + m_\eta)^2.$$
(23)

In our calculation, we use an analytical parametrization of $\sigma_{pp \to \eta pp}(s)$ motivated by Eq. (23) and given by

$$\sigma_{pp \to \eta pp}(s) = A \frac{(1 - x)^2}{\sqrt{\lambda(s, m_p^2, m_p^2)}} \left(1 + \left[\frac{b}{x}(1 - x)\right]^\gamma\right)^{-1},$$

$$x = \sqrt{\frac{s_0}{s}}, \quad A = 4 \times 10^2 \; \text{mb GeV}^2, \quad \gamma = 1.8, \; b = 17.$$
(24)

This parametrization gives an average of the estimations of Refs. [29,30] for the cross section and numerically coincides with the prediction of Ref. [31].

The η-production cross section in pn collisions near the threshold is a subject of some debate. Usually, it is assumed that this cross section should be scaled when comparing with the pp cross section, i.e., $\sigma_{pn \to \eta pn} = \kappa\sigma_{pp \to \eta pp}$. The possible increase of $\sigma_{pn \to \eta pn}$ reflects the dynamics of eta production, which is beyond our "kinematical" consideration given by Eqs. (23) and (24). But if we introduce the enhancement factor κ into $\sigma_{pn \to \eta pn}$, then approximately the same factor $[\sim (1 + \kappa)]$ should be included into the cross section of interaction of the proton with a correlated two-nucleon cluster.

The one-boson exchange model prediction of Ref. [29] is $\kappa \sim 3$. Estimation of κ within a statistical string model [32,33] gives $\kappa \sim 1$ in a wide energy range, starting from the threshold. An attempt at a direct extraction of κ from experiment near the threshold indicates a large value [34] $\kappa \sim 8$–9. Unfortunately, we have no real information on the cross section $\sigma_{pn \to \eta pn}$. On the one hand, the energy dependent one-boson exchange model parameters of Refs. [29,30] are not fixed from independent experiments. On the other hand, extracting $\sigma_{pn \to \eta pn}$ from the nuclear data one has to take carefully into account both the internal motion of the nucleons and short-range nucleon-nucleon correlations in nuclei. The latter ef-

fect increases the total cross section near the threshold strongly (about one order of magnitude), and this increase may be described phenomenologically as an increase of κ. Taking into account this indirect knowledge of $\sigma_{pn \to \eta pn}$ we adopt for the latter the same expression as for the pp case, Eq. (24) with $A = 3 \times 10^3$ mb GeV^2, $b = 33$, and $\gamma = 2.1$. The contribution of the two-nucleon correlation becomes completely negligible at bombarding energies $E \geq 1.3$ GeV. Equations (23) and (24) give the prescription for $\sigma^{(2)}_{pd \to \eta pd}(s)$ in Eq. (22). This expression has the same form $\frac{\sqrt{3}}{2}(\sigma_{pp} + \sigma_{pn})$ with the substitution $\lambda(s, m_p^2, m_p^2) \to \lambda(2s + m_p^2, 4m_p^2, m_p^2)$.

At 1 GeV, the η-production cross section taking into account only the internal nucleon motion is about 2.6×10^{-4} mb, while with the two-nucleon correlation we obtain $\sigma_{pd \to \eta}(s) \approx 5.1 \times 10^{-3}$ mb. This strong effect of the subthresold η production is seen in the dilepton distributions at initial energy 1 GeV at large invariant masses near the kinematical limit. In this case, the contribution of the η Dalitz decay is comparable with the contribution of the Δ Dalitz decay and pd bremsstrahlung, and is seen but is not dominant. So we find that the total dilepton invariant mass distribution in pd collisions at 1 GeV is not very sensitive to the large uncertainty of the eta-production cross section in pn collision, near the threshold. For higher energies (~5 GeV), we have to take into account the total inclusive eta-production cross section, which is larger than the exclusive cross section discussed above. At 4.9 GeV, we use the upper limit for the eta-production cross section [13]: 0.5 mb with $\sigma_{pp} = \sigma_{pn}$; our choice of $\kappa = 1$ corresponds to a prediction which is in agreement with the statistical string model [32].

Estimates of the ω Dalitz decay may be performed on the basis of Eq. (20) with the substitutions $\sigma_\eta \to \sigma_\omega$, $m_\eta \to m_\omega$, $m_0 \to m_\pi$, $2\alpha \to \alpha$, and $0.39 \to 0.08$. Using the known experimental data on the ω production cross section [35], we find that the contribution of the ω Dalitz decay to the dilepton production is several orders of magnitude smaller than the contribution of other subprocesses even at 5 GeV.

We do not consider the Dalitz decay of pions because it contributes to the low invariant mass region $M \leq m_\pi$ not investigated here.

V. RESULTS

In Figs. 4–7 we display our results. Invariant mass spectra for the pd reactions without and with an experimental filter are displayed in Figs. 4 and 5. The acceptance Dilepton Spectrometer (DLS) Collaboration filter we have used is version 2.0. The filter suppresses the dilepton yield at all invariant masses, and the resulting suppression is different for different subprocesses because of different kinematic conditions and kinematical limits in each channel. For comparison, we also display in Fig. 5 the results of the DLS Collaboration [3] for the p-^{9}Be interaction scaled by a factor $A_{^9Be}^{-2/3}$. If we assume that the absorption of an initial proton in a nucleus is proportional to A^{-1}, then the A dependence should be $\propto A^{2/3}$.
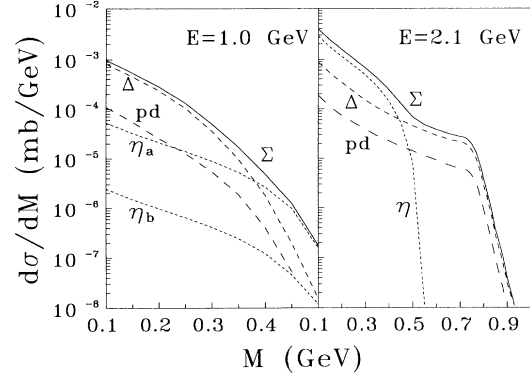
FIG. 4. Dielectron invariant mass spectra for the pN collision ($pN = pd/2$) at $E = 1.0$ and 2.1 GeV calculated without the DLS filter. The pd labels bremsstrahlung, η, Δ, and ω denote the corresponding Dalitz decay contributions, ρ/ω is the direct rho-omega decay, and Σ is the sum of all contributions. The line η_b at 1 GeV represents the subthreshold η-decay contribution taking into account the internal nucleon motion in a deuteron; the line η_a shows calculations with the two-nucleon short-range correlation.

The result of calculation in Ref. [36] shows that the absorption factor for beryllium numerically coincides with A^{-1}. This means that one can expect that the dielectron-production cross section for the p-^{9}Be interaction, scaled by a factor of $A^{-2/3}$, may be considered approximately as dilepton production in a p-isoscalar nucleon interaction. Other medium effects (excluding internal motion) in the light beryllium nucleus are expected to be negligible. Therefore one must consider the scaled beryllium data as some rough guide of what is to be expected by proper pd data at 1–2 GeV. We do not attempt a fine tuning of our input to reproduce exactly the scaled data.

In calculating the Δ Dalitz decay and bremsstrahlung
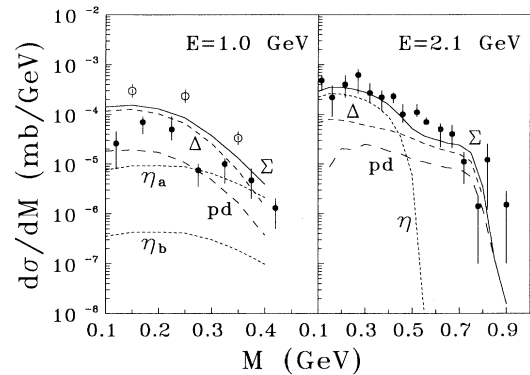
FIG. 5. Dielectron invariant mass spectra for the pN collision at $E = 1.0$ and 2.1 GeV calculated with the DLS filter. Notations for the curves are the same as in Fig. 4. Experimental data for p-^{9}Be collisions, scaled by the factor $A^{-2/3}$, are taken from Ref. [3] (solid circles). Open circles at 1 GeV represent the product of calculated dielectron yield in pp collisions and the ratio of the pd to pp dielectron production (see the text).
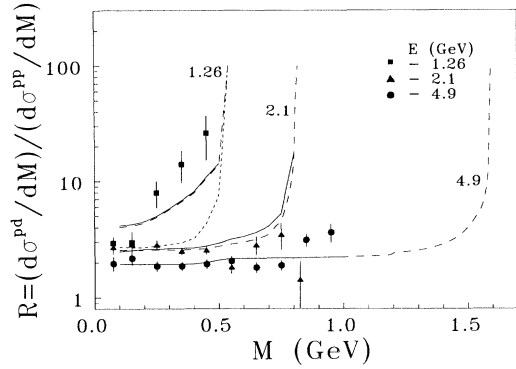
FIG. 6. Ratio of the cross section for pd to pp reactions at $E = 1.26, 2.1$, and 4.9 GeV. The short dashed line at $E = 1.26$ GeV corresponds to the calculation without eta-decay contribution in pd collision. The experimental data are taken from Refs. [2,37]. Dashed and solid lines correspond to the calculation with and without the DLS filter, respectively.

contribution in pd reactions, we also take into account the internal motion of nucleons in the deuteron, as in Eq. (21). The integrations in Eqs. (1), (13), and (21) are performed by a Monte Carlo method. The cross section of the elastic scattering in Eq. (13) is parametrized to reproduce the experimental data at each initial energy separately.

Our results for 1 and 2 GeV without the DLS filter are close numerically to the results of our previous paper [12], where the above-mentioned off-shell suppression has been used. A small difference is explained by different parametrization of the η-production cross section (in Ref. [12] the prediction of Ref. [29] was used) and taking into account in Ref. [12] the phenomenological off-shell correction in the two-body T matrix in the bremsstrahlung channel. In Ref. [12], antisymmetrization in the pd collision was somehwat overestimated. At 2 GeV, the bremsstrahlung is not a dominant source of the dileptons, and the off-shell effect is not seen in the total cross section. At 1 GeV, the effect of the off-shell
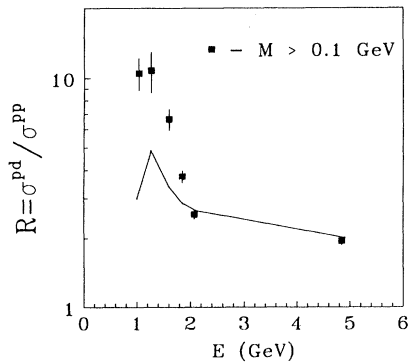
FIG. 7. Ratio of the integrated cross section for pd to pp reactions as function of the initial energy. Solid line corresponds to the calculation with the DLS filter. The experimental data are taken from Refs. [2,37].

correction is much smaller. So concerning the off-shell effects our present result may be considered as an upper limit for the bremsstrahlung contribution.

In Figs. 4 and 5 we present the results of calculation without and with the DLS acceptance filter. As a matter of fact, our study shows that the influence of the DLS filter is much stronger than the off-shell corrections discussed in Ref. [12] and it is strictly necessary to take the filter into account for a correct comparison with experimental data.

At 1 GeV, we find the bremsstrahlung contribution nearly as strong as the Δ Dalitz decay. There is also a contribution of the η Dalitz decay. Near the threshold the η decay gives the same (or even) larger contribution than the Δ Dalitz decay and bremsstrahlung. Subthreshold effects are responsible for larger invariant mass tails of the Δ and bremsstrahlung contributions in the pd reactions. The vector dominance effects (i.e., the form factor) are not important.

In contrast, at 2.1 GeV the VDM effect is important. However, the strong enhancement of the Δ Dalitz decay at the ρ peak is reduced by the t dependence of the delta-production matrix element. The net result is a shoulder in the sum of all contributions. This is not so clearly seen in pp reactions due to the kinematic limit. However, in pd reactions, due to subthreshold effects, it can be observed. Our net results are of the same order of magnitude as those obtained in Ref. [6], but in Ref. [6] there is no shoulder behavior in the ρ region. In the intermediate invariant mass region $0.2 \leq M \leq 0.4$ GeV the η Dalitz decay gives the main contribution. The contribution of the ω Dalitz decay is very small and is not displayed here.

A similar analysis of the dilepton production in the proton-nucleon collision taking into account proton-nucleon bremsstrahlung and the effect of propagating the Δ resonance (Δ Dalitz decay) has been performed in [16]. The principal results of those two channels in Ref. [16] and in our study coincide, i.e., the main contribution to the dilepton spectrum comes from the Δ decay. But there is some difference in the interpretation of the pd/pp ratio. In Ref. [16], some enhancement of the ratio at lower energies may be explained by (i) different values of the Δ-production cross section (in Ref. [16] this difference is by the factor 2–3) and (ii) a relatively large destructive interference between bremsstrahlung and the Δ-decay channel in pp as compared to the pn collisions. In our model, the first effect exists but its contribution is smaller. The difference between the Δ-production cross sections is controlled by the Ver West–Arndt parametrization and it is by a factor of ~ 1.7 at $E = 1.2$ GeV. The second effect is dropped here; however, we take into account the η-decay contribution.

Now let us consider the ratio of the cross section for pd to pp reactions,

$$R = \frac{d\sigma^{pd}/dM}{d\sigma^{pp}/dM}, \tag{25}$$

which is displayed in Fig. 6 for three energies $E = 1.26$, 2.1, and 4.9 GeV. The experimental data are taken from Ref. [2].

It should be pointed out that at 4.9 GeV we calculated $d\sigma^{pd}/dM$ and $d\sigma^{pp}/dM$ in Eq. (25) within the same models as at lower energies. We did not take into account the following important channels with multipion final states: bremsstrahlung, delta Dalitz decay, pion annihilation, etc., and as a result, we underestimated the experimental cross section (Ref. [1]) at $M = 0.2-0.7$ GeV by the factor of 2-4. But we expect that those additional channels should be the same in pp and pd collisions and their absence in our calculation does not change the ratio.

The difference between pp and pd interactions consists in (i) taking into account the internal nucleon motion in a deuteron, (ii) different expressions for the Δ-production cross section which follow from the Ver West–Arndt parametrization in Eq. (12), and (iii) the absence of the η-decay contribution in the pp case above the threshold. If the bremsstrahlung contribution in the pp and pd collisions were switched off and the eta-production cross section in the pn reaction taken equal to the cross section in the pp collision, the ratio would be energy independent and close to 2 except for the vicinity of the kinematic pp threshold. It is seen that the ratio rises towards the kinematic limits due to phase space limitations in the pp reactions. Except for this boundary behavior, the ratio decreases towards 2 with increasing initial energy, which reflects the decrease of the difference between η Dalitz decay contribution in proton-proton and proton-neutron collisions, and relative decrease of the short-range correlation effect responsible for the sub-threshold η-production elastic NN-scattering cross section. At 1.26 GeV, the result is very sensitive to the sub-threshold η-production mechanism. The effect of the sub-threshold η production is illustrated by the short dashed line in Fig. 6, which corresponds to the calculation without eta-decay contribution in pd collision at $E = 1.26$ GeV. To summarize, we can conclude that at $E = 1.26$ GeV and $M \sim 0.2 - 0.3$ GeV, in spite of qualitative agreement with data, the theoretical prediction with the eta-decay channel is about twice smaller than the data.

Our analysis shows that for the pp collision at 1 GeV only the Δ Dalitz and pp bremsstrahlung contribute. Theoretical uncertainties in the pp interaction are minimal because the total and differential Δ-production cross sections at 1 GeV are well known, as well as the elastic pp cross section operating in bremsstrahlung. So the calculated dielectron-production cross section for the pp collision being multiplied by an experimentally measured quantity R results in an estimation for dielectron yield in the pd collision at 1 GeV [cf. Eq. (25)]. The corresponding points are shown in Fig. 5 (open circles).

Figure 7 shows the ratio of the integrals

$$R_{int} = \frac{\int_{0.1 \text{ GeV}}^{M_{max}} (d\sigma^{pd}/dM)dM}{\int_{0.1 \text{ GeV}}^{M_{max}} (d\sigma^{pp}/dM)dM} \quad (26)$$

as a function of the initial energy E with the DLS filter. One can see some enhancement of the ratio at $E < 1.4$ GeV because of the large sub- (and near-) threshold η Dalitz decay contribution in the pd collisions and pn bremsstrahlung contribution. Again, one can see the difference of the factor 2 between prediction and the data and the origin of this difference is the same as in Fig. 6. Then the ratio goes to 2 as the contribution of the main channels in the pp and pn collisions becomes the same. If we switch off the eta-decay channel than the bump in this ratio disappears.

VI. SUMMARY

In summary, we present a detailed analysis of dielectron production in the pp and pd reactions at 1–2 GeV. Our model relies on vector dominance, improves the soft photon approximation, and uses the correct Δ-production cross section. We explain the observed strong enhancement of the ratio of dielectron production in pd and pp collisions at 1–1.3 GeV. We show that an additional and large enough contribution to the pp/pd ratio at low energies comes from the eta Dalitz decay, and we show that the enhancement may be understood by different threshold behavior of the eta production in proton-proton and proton-neutron collisions.

We can conclude that the dilepton-production cross section is sensitive to the very details of the elementary subprocesses which have been analyzed. The accuracy of the Δ, η, ω Dalitz and direct ρ, ω decays depends on the knowledge of the unstable hadron production mechanisms. So new precision measurements in the Bevalac, SIS, COSY energy region are needed. Also, an independent verification of the two-body T matrix off-shell behavior and timelike nucleon form factor is needed. Only a clear understanding of the dilepton production in NN interaction can give a reliable possibility to use dileptons as an accurate probe for a more complex nuclear collision.

ACKNOWLEDGMENTS

[1] H. Z. Huang et al., Phys. Lett. B 297, 233 (1992); Phys. Rev. C 49, 314 (1994).

[2] W. K. Wilson, et al., Phys. Lett. B 316, 245 (1994); Report No. LBL 33625, Berkeley, 1993.

[3] G. Roche et al., Phys. Rev. Lett. 61, 1069 (1988); Phys. Lett. B 226, 228 (1989); C. Naudet, et al., Phys. Rev. Lett. 62, 2652 (1989).

[4] C. Gale and J. Kapusta, Phys. Rev. C 35, 2107 (1987).

[5] C. Gale and J. Kapusta, Phys. Rev. C **40**, 2397 (1989).

[6] G. Wolf, G. Batko, W. Cassing, U. Mosel, K. Niita, and M. Schäfer, Nucl. Phys. **A517**, 615 (1990).

[7] L. Xiong, Z. G. Wu, C. M. Ko, and J. Q. Wu, Nucl. Phys. **A512**, 772 (1990).

[8] K. K. Gudima, V. D. Toneev, and A. I. Titov, Phys. Lett. B **287**, 302 (1992).

[9] L. A. Winckelmann, H. Stöcker, W. Greiner, and H. Sorge, Phys. Lett. B **298**, 22 (1993).

[10] M. Schäfer, T. S. Biro, W. Cassing, and U. Mosel, Phys. Lett. B **221**, 1 (1989).

[11] K. Haglin, J. Kapusta, and C. Gale, Phys. Lett. B **224**, 433 (1989); **221**, 1 (1989).

[12] B. Kämpfer, A. I. Titov, and E. L. Bratkovskaya, Phys. Lett. B **301**, 123 (1993).

[13] K. Haglin and C. Gale, Phys. Rev. C **49**, 401 (1994).

[14] G. Wolf, W. Cassing, and U. Mosel, Nucl. Phys. **A545**, 139c (1992).

[15] J. J. Sakurai, *Currents and Mesons* (University of Chicago Press, Chicago, 1969).

[16] M. Schäfer, H. C. Dönges, A. Engel, and U. Mosel, Nucl. Phys. **A575**, 429 (1994).

[17] A. M. Eisner, E. L. Hart, R. I. Louttit, and T. W. Morris. Phys. Rev. **138**, B670 (1965).

[18] S. Colletti *et al.*, Nuovo Cimemto **49**, 479 (1967).

[19] G. F. Bertsch, G. E. Brown, V. Koch, and B. A. Li, Nucl. Phys. **A490**, 745 (1988).

[20] H. F. Jones and M. D. Scadron, Ann. Phys. (N.Y.) **81**, 1 (1973).

[21] B. J. Ver West and R. A. Arndt, Phys. Rev. C **25**, 1979 (1982).

[22] K. Haglin, Ann. Phys. (N.Y.) **212**, 84 (1991).

[23] E. L. Bratkovskaya, B. L. Reznik, and A. I. Titov, Sov. J. Nucl. Phys. **55**, 3058 (1992).

[24] Particle Data Group, J. J. Hernández *et al.*, Phys. Lett.

B **239**, 1 (1990).

[25] M. Lacombe, B. Loiseau, J. M. Richard, and R. Vinh Mau, Phys. Rev. C **21**, 861 (1980).

[26] L. P. Kaptari, B. L. Resnik, and A. I. Titov, Sov. J. Nucl. Phys. **42**, 777 (1985); A. V. Efremov, Sov. J. Part. Nucl. **13**, 254 (1982); V. V. Burov, S. M. Dorkin, V. K. Lukyanov, and A. I. Titov, Z. Phys. A **306**, 149 (1982).

[27] H. Pirner and J. P. Vary, Phys. Rev. Lett. **46**, 1376 (1981).

[28] T. Fujita. Phys. Rev. Lett. **39**, 174 (1977); Phys. Lett. **72B**, 16 (1977).

[29] T. Vetter, A. Engel, T. Biro, and U. Mosel, Phys. Lett. B **263**, 153 (1991).

[30] J. M. Laget, F. Wellers, and J. F. Lecolley, Phys. Lett. B **257**, 254 (1991).

[31] A. L. De Paoli, K. Niita, W. Cassing, U. Mosel, and C. M. Ko, Phys. Lett. B **219**, 194 (1989).

[32] N. S. Amelin, K. K. Gudima, S. Yu. Sivoklokov, and V. D. Toneev, Sov. J. Nucl. Phys. **52**, 272 (1990).

[33] V. D. Toneev, A. I. Titov, and K. K. Gudima, Report No. GSI-92-05, 1992.

[34] E. Chiavassa, G. Dellacasa, N. De Marco, F. Ferrero, M. Gallio, A. Musso, A. Piccotti, E. Scomparin, E. Vercellin, J. M. Durand, and P. Fassnacht, Z. Phys. A **344**, 345 (1993); Phys. Lett. B **322**, 270 (1994).

[35] V. Flaminio, W. G. Moorhead, D. R. O. Morrison, and N. Rivoire, Report No. CERN-HERA 84-01 (data compilation), 1984.

[36] L. P. Kaptari, V. K. Lukyanov, B. L. Resnik, and A. I. Titov, in *Relativistic Nuclear Physics and Quantum Chromodynamics*, edited by A. M. Baldin *et al.* (World Scientific, Singapore, 1991), p. 355.

[37] G. Roche, Report No. PCCF RI 9316, Université Blaise Pascal, 1993.